New Journal of Physics

The open access journal at the forefront of physics

PAPER

Curing Braess' paradox by secondary control in power grids

Eder Batista Tchawou Tchuisseu[1] ⓘ , Damià Gomila[1] ⓘ , Pere Colet[1] ⓘ , Dirk Witthaut[2,3] ⓘ ,
Marc Timme[4,5] ⓘ and Benjamin Schäfer[4,5] ⓘ

1   Instituto de Física Interdisciplinar y Sistemas Complejos, IFISC (CSIC-UIB), Campus Universitat Illes Balears, E-07122 Palma de Mallorca, Spain
2   Forschungszentrum Jülich, Institute for Energy and Climate Research—Systems Analysis and Technology Evaluation (IEK-STE), D-52428 Jülich, Germany
3   Institute for Theoretical Physics, University of Cologne, D-50937 Köln, Germany
4   Chair for Network Dynamics, Center for Advancing Electronics Dresden (cfaed) and Institute for Theoretical Physics, Technical University of Dresden, D-01062 Dresden, Germany
5   Network Dynamics, Max Planck Institute for Dynamics and Self-Organization (MPIDS), D-37077 Göttingen, Germany

E-mail: benjamin.schaefer@tu-dresden.de

Keywords: control, stability, power grid, Braess' paradox, smart grid

Abstract

The robust operation of power transmission grids is essential for most of today's technical infrastructure and our daily life. Adding renewable generation to power grids requires grid extensions and sophisticated control actions on different time scales to cope with short-term fluctuations and long-term power imbalance. Braess' paradox constitutes a counterintuitive collective phenomenon that occurs if adding new transmission line capacity to a network increases loads on other lines, effectively reducing the system's performance and potentially even entirely destabilizing its operating state. Combining simple analytical considerations with numerical investigations on a small sample network, we here study dynamical consequences of secondary control in AC power grid models. We demonstrate that sufficiently strong control not only implies dynamical stability of the system but may also cure Braess' paradox. Our results highlight the importance of demand control in conjunction with the grid topology to ensure stable operation of the grid and reveal a new functional benefit of secondary control.

1. Introduction

Modern electrical power grids are complex interconnected networks in which supply and demand have to match at all times since the grid itself cannot store any energy [1, 2]. To guarantee this match, different economic mechanisms, like day-ahead and intra-day markets are used [3]. For unscheduled mismatches, e.g. random fluctuations [4], disturbances or extreme weather, faster control mechanisms are required [5]. Such control actions become increasingly important due to the rising share of renewable generation integrated into the grid [6–8]. Control mechanisms are ordered by their time scale on which they act: suppose a power plant has to unexpectedly shut down and all of a sudden there is a shortage of power in the system. The first second of the disturbance is mainly uncontrolled, i.e. energy is drawn from the spinning reserve of the generators. Within the next seconds, the primary control sets in to stabilize the frequency and to prevent a large drop. To restore the frequency back to its nominal value of 50 or 60 Hertz, secondary control is necessary [5]. However, in many recent studies on power system dynamics and stability, the effects of control are completely neglected or only primary control is considered [9–16]. Including secondary control might be crucial when determining stability conditions. Even in cases where secondary control is modeled explicitly [17], its stability properties and interaction with the network topology are typically not fully investigated.

Nonetheless, grid topology and control mechanisms have to adapt within the next years to cope with the spatially distributed and fluctuating renewable generation. Grid adaptation includes additional transmission lines, e.g., to connect distant renewable generators [18], and increasing capacity of existing lines [19, 20], e.g. to prevent cascading failures [21]. Contrary to expectations, not all added lines are beneficial to the stability of a

grid. Instead, adding some lines may cause the grid to lose its operating state via Braess' paradox, which was initially discovered for transportation networks [22] but may also occur in power grids [23–27].

Here, we present a dynamical analysis on the effectiveness and limitations of an implementation of secondary control that depends on the voltage phase angle θ of a synchronous machine. We dynamically show how a simple implementation of secondary control restores a grid with a power mismatch back to the nominal frequency. Furthermore, we investigate the stability of a grid with secondary control as a function of the network topology. In particular, we find that secondary control reliably prevents Braess' paradox if all nodes are controlled. However, controlling only generators still allows Braess' paradox as before, thereby highlighting the importance of demand-side control in future grids.

This article is structured as follows. First, we introduce a simple model of the dynamics of the electric power network in the presence of secondary control in section 2. Next, we present a stability analysis of the grid with secondary control in section 3. Section 4 demonstrates the effectiveness of secondary control in the elementary two-node system. Finally, we investigate how secondary control may prevent Baress' paradox by controlling all machines (section 5) and how it is limited when only controlling generators (section 6). We close the paper with a discussion on the impact of our results on current and future power grids.

2. Mathematical modeling of the electric power system

The electric power grid may be modeled as an interconnected network consisting of nodes linked by power transmission lines (links). Each node in this coarse-grained model represents a local area including power generation and consumption with net mechanical power input P_i^{m} being negative for effective consumer regions, e.g. urban areas, and positive for effective generators. Let f_R be the reference frequency of the power grid (50 or 60 Hz) and $\omega_R = 2\pi f_R$ be the reference angular velocity. We model each node by the well-known *swing equation* [1, 5, 9, 10, 15, 28], which in the reference frame rotating at ω_R, is given by

$$\dot{\theta}_i = \omega_i, \tag{1}$$

$$\dot{\omega}_i = \frac{\omega_R}{2H_i P_i^{\mathrm{G}}}(P_i^{\mathrm{m}}(\omega_i) - P_i^{\mathrm{e}}(\theta_i, \omega_i)). \tag{2}$$

The state of node i is characterized in the co-moving reference frame by the voltage phase angle θ_i and the angular velocity deviation ω_i. H_i is the inertia constant of the generator with a nominal capacity P_i^{G}. Due to the choice of the reference frame, $\omega_i = 0$ implies that the node is operating at the reference frequency f_R. P_i^{e} represents the total power consumed and transmitted at node i:

$$P_i^{\mathrm{e}}(\theta_i, \omega_i)) = \left(1 + \frac{D_i}{\omega_R}\omega_i\right)P_i^{\mathrm{l}} + \sum_{j=1}^{n} B_{ij}\sin(\theta_i - \theta_j), \tag{3}$$

where P_i^{l} is the load dissipated when the frequency is f_R and D_i determines the fraction of the load that is frequency dependent, for instance electrical motors or damper windings. The last term gives the power transmitted from node i to other nodes with B_{ij} being proportional to the susceptance of line (i, j).

The power grid is subject to fluctuations, e.g. due to changing demand, volatile generation of renewables or trading [4, 28–30]. To cope with these fluctuations, the grid is controlled on multiple time scales with primary control being the fastest, followed by secondary control [31]. The primary frequency control adjusts the mechanical power output proportional to the angular velocity deviation ω_i [5, 32],

$$\dot{P}_i^{\mathrm{m}} = \frac{1}{\tau_i}\left[P_i^{\mathrm{s}} - P_i^{\mathrm{m}} - \frac{P_i^{\mathrm{G}}}{R_i \omega_R}\omega_i\right], \tag{4}$$

where τ_i is the characteristic response time of the primary control, P^{s} is the spinning reserve power and R_i is the governor speed regulation. Secondary control is then applied through automatic generation control to restore the frequency,

$$\dot{P}_i^{\mathrm{s}} = -\frac{\kappa_i}{\omega_R}\omega_i, \tag{5}$$

where κ_i is the gain parameter of the secondary control. Integrating equation (5) gives

$$P_i^{\mathrm{s}}(t) = -\frac{\kappa_i}{\omega_R}\theta_i(t) + P_i^{\mathrm{ref}}, \tag{6}$$

where P_i^{ref} is the nominal spinning power. Introducing relation (6) into equations (3) and (4) and defining $P_i = \frac{\omega_R}{2H_i P_i^{\mathrm{G}}}(P_i^{\mathrm{ref}} - P_i^{\mathrm{l}}), (0), \alpha_i = \frac{D_i}{2H_i P_i^{\mathrm{G}}}P_i^{\mathrm{l}}, \beta_i = \frac{1}{2R_i H_i}, \gamma_i = \frac{\kappa_i}{2H_i P_i^{\mathrm{G}}}$ and $K_{ij} = \frac{\omega_R}{2H_i P_i^{\mathrm{G}}}B_{ij}$ one obtains:

$$\dot{\theta}_i = \omega_i, \tag{7}$$

$$\dot{\omega}_i = -\alpha_i \omega_i + P_i - \sum_{j=1}^{n} K_{ij} \sin(\theta_i - \theta_j) + P_i^c, \tag{8}$$

$$\tau_i \dot{P}_i^c = -P_i^c - [\beta_i \omega_i(t) + \gamma_i \theta_i]. \tag{9}$$

Here α_i plays the role of an effective damping constant and P_i is the net power fed into the grid or consumed at node i, i.e., P_i is positive for effective generators, while it is negative for effective consumers. K_{ij} determines the capacity of a line, P_i^c is the control power with time constant τ_i, while β_i and γ_i essentially give the magnitude of the primary and secondary control respectively. Equations (7) and (8) have the form of the well-known 2nd-order Kuramoto model, which has been used for example in [9, 33] without control to describe the dynamics of the power grid.

In the remainder of this article, we set the parameter $\tau_i = 0$, meaning that the control acts instantaneously. This approximation does not affect the final steady state of the system, which we are mainly interested in, simplifying the model considerably. The time constant τ_i only changes the frequency of the oscillations during the transient dynamics. Thereby, we can solve equation (9) for P^c and insert it into equation (8). In addition, since the damping α_i and primary control β_i play a similar dynamical role, we absorb any contribution from β_i into α_i, effectively setting $\beta_i = 0$. With that, our equation of motion for each node reads

$$\dot{\theta}_i = \omega_i,$$
$$\dot{\omega}_i = -\alpha_i \omega_i - \gamma_i \theta_i + P_i - \sum_{j=1}^{n} K_{ij} \sin(\theta_i - \theta_j). \tag{10}$$

The control term $-\gamma_i \theta_i$ has the same form as the integral control used in [17]. Alternative control schemes have been considered in [17, 34–38].

Throughout this article, we will initialize numerical simulations of the set of equations (10) using $\theta_i(0) = 0$ and $\omega_i(0) = 0$ for all nodes.

3. Steady state analysis and stability condition

The power grid is in a steady state if all rotatory machines are phase-locked, i.e, have the same frequency, which ideally is the reference frequency of $f_R = 50$ or 60 Hz [39]. Mathematically, the phase-locked state is a fixed point of (10) which is given by $\omega_i^* = 0$ and

$$\sum_{j=1}^{N} K_{ij} \sin(\theta_i^* - \theta_j^*) = P_i - \gamma_i \theta_i^*, \tag{11}$$

for all $i = 1, \ldots, N$. Without control, $\gamma_i = 0$, these algebraic equations do not always have a solution for the phases θ_i^*. As a trivial example, without enough transmission capacity, i.e, $\sum_{j=1}^{N} K_{ij} < P_i$ for finite power $P_i \neq 0$ there cannot be any fixed point. However, when control is included in all nodes $\gamma_i > 0$, $\forall i$ then there is always at least one fixed point solution [17].

To derive the stability conditions of the synchronous state with respect to small perturbations, we linearize equation (10) around (θ_i^*, ω_i^*). We denote small perturbations around the fixed point as $\theta_i = \theta_i^* + \delta\theta_i$ and $\omega_i = \omega_i^* + \delta\omega_i$ and define $\mathbf{X_1}$ and $\mathbf{X_2}$, as the n-dimensional vectors of $\delta\theta_i$ and $\delta\omega_i$, respectively. Linearizing (10) yields

$$\dot{\mathbf{X}}_1 = \mathbf{X}_2,$$
$$\dot{\mathbf{X}}_2 = -(\mathbf{L} + \mathbf{\Gamma})\mathbf{X}_1 - \mathbf{A}\mathbf{X}_2, \tag{12}$$
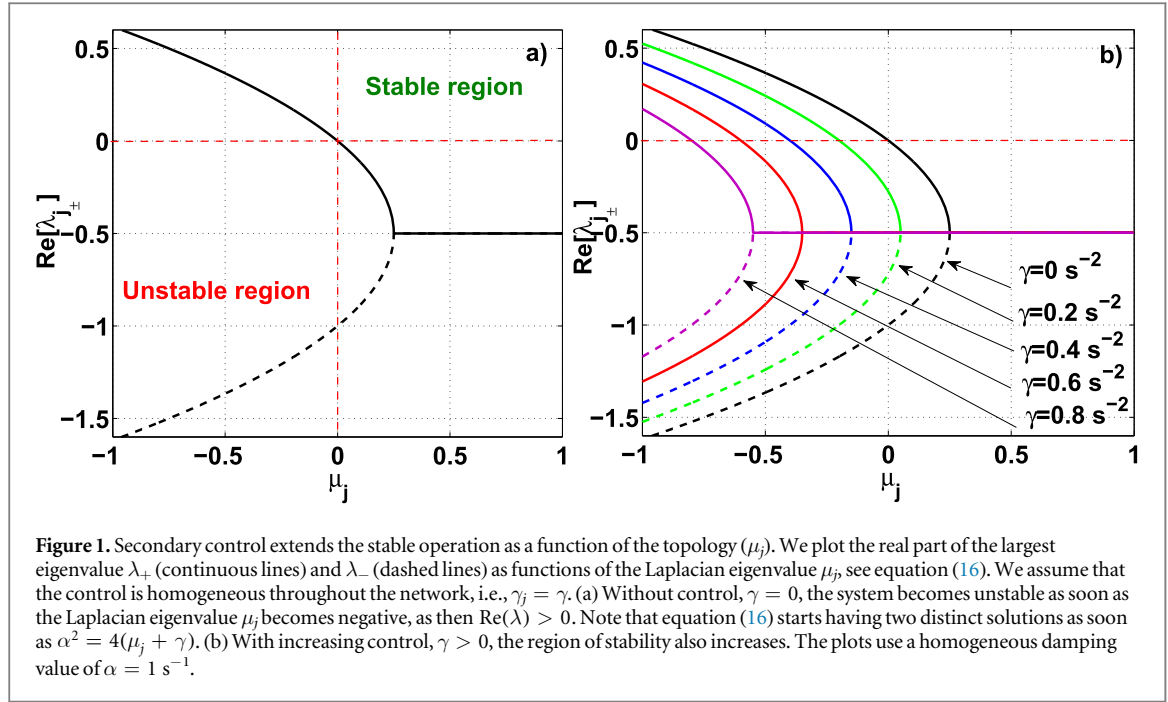
where $\mathbf{\Gamma}$ and $\mathbf{A}$ are diagonal matrices with elements $\Gamma_{ii} = \gamma_i$ and $A_{ii} = \alpha_i$ respectively, representing the control and the damping matrix. Matrix $\mathbf{L} = (L_{ij})$ is a Laplacian matrix of the network topology, defined as

$$L_{ij} = \begin{cases} -K_{ij} \cos(\theta_i^* - \theta_j^*), & i \neq j, \\ -\sum_{l \neq i}^{n} L_{il}, & i = j. \end{cases} \tag{13}$$

The Lyapunov exponents $\{\lambda_j\}$ of the dynamical system (12) are given by the eigenvalues of the Jacobian matrix

$$\mathbf{J} = \begin{bmatrix} \mathbf{0} & \mathbf{1} \\ -\mathbf{L} - \mathbf{\Gamma} & -\mathbf{A} \end{bmatrix}. \tag{14}$$

Without secondary control, i.e., $\gamma = 0$, there is a single zero Lyapunov exponent which arises because the stability is only defined up to an arbitrary phase shift, i.e., we could replace all phases by adding a constant

Figure 1. Secondary control extends the stable operation as a function of the topology (μ_j). We plot the real part of the largest eigenvalue λ_+ (continuous lines) and λ_- (dashed lines) as functions of the Laplacian eigenvalue μ_j, see equation (16). We assume that the control is homogeneous throughout the network, i.e., $\gamma_j = \gamma$. (a) Without control, $\gamma = 0$, the system becomes unstable as soon as the Laplacian eigenvalue μ_j becomes negative, as then $\text{Re}(\lambda) > 0$. Note that equation (16) starts having two distinct solutions as soon as $\alpha^2 = 4(\mu_j + \gamma)$. (b) With increasing control, $\gamma > 0$, the region of stability also increases. The plots use a homogeneous damping value of $\alpha = 1 \text{ s}^{-1}$.

everywhere $\theta_i \to \tilde{\theta}_i = \theta_i + \text{const.}$ [13]. In this case the synchronous state is stable if the real part of the other Lyapunov exponents is negative.

The inclusion of secondary control breaks the phase invariance and, as a consequence, for $\gamma > 0$, there is no generic zero Lyapunov exponent, except at bifurcation points. Hence, the synchronous state of the system is stable if and only if the real part of all Lyapunov exponents is negative.

In the case in which the damping and control parameters are the same for all nodes, namely $\alpha_i = \alpha$ and $\gamma_i = \gamma$, the stability of the synchronized state can be analyzed using the master stability function technique [40]. We diagonalize the Laplacian matrix **L** by substituting $\mathbf{Y_1} = \mathbf{M}^{-1}\mathbf{X_1}$, $\mathbf{Y_2} = \mathbf{M}^{-1}\mathbf{X_2}$, where **M** is the matrix composed of the eigenvectors of **L** such that that $\mathbf{\Lambda} = \mathbf{MLM}^{-1}$ is the diagonalized matrix composed by the eigenvalues of **L** μ_j. We assume symmetric coupling $K_{ij} = K_{ji}$, thereby guaranteeing real eigenvalues μ_j. Equation (12) can be rewritten as

$$\frac{d}{dt}\begin{bmatrix} Y_{1j} \\ Y_{2j} \end{bmatrix} = \begin{bmatrix} 0 & 1 \\ -\mu_j - \gamma & -\alpha \end{bmatrix}\begin{bmatrix} Y_{1j} \\ Y_{2j} \end{bmatrix}. \tag{15}$$

The Lyapunov exponents are given by:

$$\lambda_{j\pm} = -\frac{\alpha}{2} \pm \frac{1}{2}\sqrt{\alpha^2 - 4(\mu_j + \gamma)}. \tag{16}$$

Without control, $\gamma = 0$, stability is guaranteed if all eigenvalues μ_j of the Laplacian matrix are positive, see equation (16) and [11, 13]. If however a given eigenvalue μ_j is negative, one of the corresponding eigenvalues $\lambda_{j\pm}$ is positive and the other one is negative; therefore, the synchronous state is unstable. With added secondary control, i.e., $\gamma > 0$, the region of stability increases, see figure 1, where we plot the real part of Lyapunov exponents $\text{Re}[\lambda_{j\pm}]$ as a function of μ_j. Mathematically, the system is stable within the region defined by $\mu_j + \gamma > 0$, see also [11, 41].

The eigenvalues $\{\mu_j\}$ depend on the topology of the network. Changing the capacity of a line, adding additional lines or removing them will change the values of $\{\mu_j\}$ and thus change $\{\lambda_j\}$, potentially leading to instabilities. In the following, we denote the non-zero Lyapunov exponent with the largest real part as λ^m and the corresponding eigenvalue of **L** as μ^m.

4. Two-node system

Let us now investigate the elementary system consisting of two nodes, a generator ($P_1 > 0$) and a consumer ($P_2 < 0$) first without secondary control to then investigate the benefits of adding such control.

4.1. Uncontrolled two-node system

Without control, $\gamma_1 = \gamma_2 = 0$, and assuming homogeneous damping $\alpha_1 = \alpha_2 = \alpha$, the dynamics is given by the following equations for the phase difference $\Delta\theta = \theta_1 - \theta_2$ and the frequency difference $\dot{\Delta\theta} = \omega_1 - \omega_2 = \Delta\omega$ with $\Delta P = P_1 - P_2$:

$$\dot{\Delta\theta} = \Delta\omega,$$
$$\dot{\Delta\omega} = -\alpha\Delta\omega + \Delta P - 2K\sin(\Delta\theta). \tag{17}$$

The system has a steady state if and only if $2K \geqslant \Delta P$, see also [13]. The physical reason for the absence of a fixed point for $2K < \Delta P$ is that the electric power flowing through a line cannot exceed the maximal capacity K.

For $2K > \Delta P$ the two steady states, T_1 and T_2, obtained from (17), and their respective eigenvalues are

$$T_1 : \begin{cases} \Delta\theta^* = \arcsin\left(\dfrac{\Delta P}{2K}\right), \ \Delta\omega^* = 0, \\[2mm] \lambda_\pm(T_1) = -\dfrac{\alpha}{2} \pm \sqrt{\dfrac{\alpha^2}{2} - \sqrt{4K^2 - \Delta P^2}}, \end{cases} \tag{18}$$

$$T_2 : \begin{cases} \Delta\theta^* = \pi - \arcsin\left(\dfrac{\Delta P}{2K}\right), \ \Delta\omega^* = 0, \\[2mm] \lambda_\pm(T_2) = -\dfrac{\alpha}{2} \pm \sqrt{\dfrac{\alpha^2}{2} + \sqrt{4K^2 - \Delta P^2}}. \end{cases} \tag{19}$$

The steady state T_1 is a stable fixed point since we assume the damping α to be positive. In contrast, the steady state T_2 is a saddle since its eigenvalues λ_+ is a positive real number.

For $2K = \Delta P$, T_1 and T_2 collide via a saddle node bifurcation on a cycle (SNIC), entering a limit cycle for $K < \frac{\Delta P}{2}$. Such limit cycles often cause large frequency deviations that would result in the shut down of (parts of) the grid and are therefore undesirable [13]. But even for sufficient transmission capacity, i.e. $2K \geqslant \Delta P$, the grid enters a limit cycle if we have unbalanced power, $P_1 + P_2 \neq 0$ so that, from equation (10) the synchronous angular velocity is given as

$$\omega_{\text{syn}} = \frac{P_1 + P_2}{2\alpha}. \tag{20}$$

Hence, the grid is no longer at its reference frequency of $f_R = 50$ or 60 Hz but below it for $P_1 + P_2 < 0$ and above it for $P_1 + P_2 > 0$. To restore the frequency to the reference, we apply our secondary controller in the next subsection.
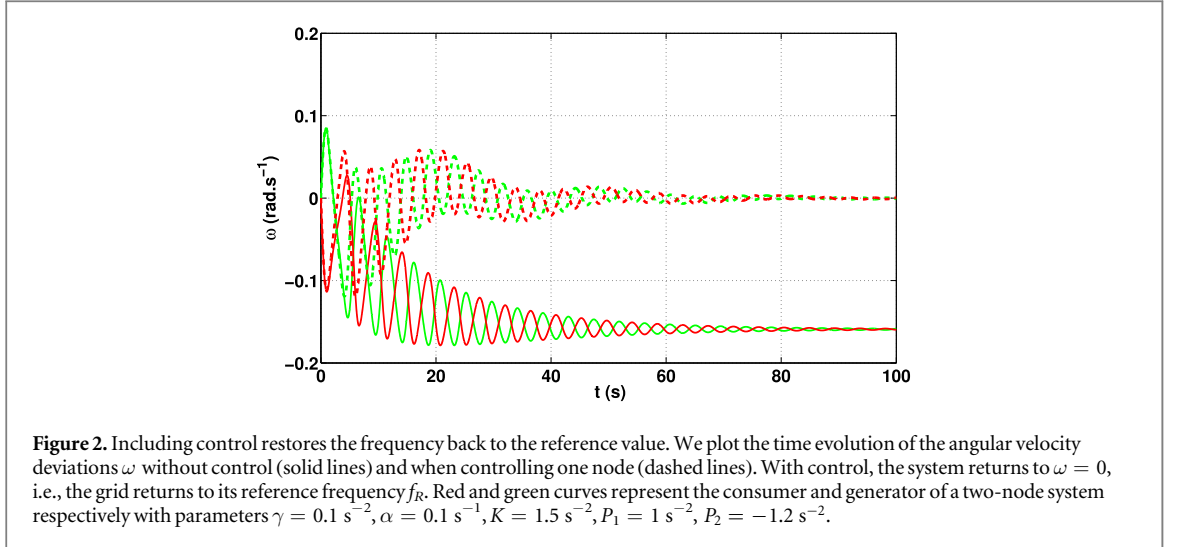
4.2. Two-node system with secondary control

Next, we consider the two-node system where one node applies a secondary control, i.e., we set the control parameters $\gamma_1 = 0$ and $\gamma_2 = \gamma$ in the equation of motion (10). Then, the steady state of the controlled system is obtained as

$$\theta_1^* = \frac{P_1 + P_2}{\gamma} + \arcsin\left(\frac{P_1}{K}\right),$$
$$\theta_2^* = \frac{P_1 + P_2}{\gamma},$$
$$\omega_1^* = 0,$$
$$\omega_2^* = 0.$$

For $P_1 > K$, there is no steady state and the system approaches a limit cycle, as the power cannot be transferred via the line and node 1 is uncontrolled. For $P_1 < K$ however, there will be a fixed point, even if the power is unbalanced $P_1 + P_2 \neq 0$, in contrast to the uncontrolled system (figure 2). While the uncontrolled system (solid lines) approaches a limit cycle with ω_{sync}, as obtained by equation (20), the controlled system is attracted to the fixed point, i.e. a stable operating state of the grid.

Next, we perform a stability analysis of the fixed point. Let $\mathbf{X} = (\delta\theta_1, \delta\theta_2, \delta\omega_1, \delta\omega_2)$ be a small perturbation of the fixed point. The equations of motion of these small perturbations are given by

$$\dot{\mathbf{X}}(t) = \mathbf{D} \cdot \mathbf{X}(t), \tag{21}$$

Figure 2. Including control restores the frequency back to the reference value. We plot the time evolution of the angular velocity deviations ω without control (solid lines) and when controlling one node (dashed lines). With control, the system returns to $\omega = 0$, i.e., the grid returns to its reference frequency f_R. Red and green curves represent the consumer and generator of a two-node system respectively with parameters $\gamma = 0.1$ s^{-2}, $\alpha = 0.1$ s^{-1}, $K = 1.5$ s^{-2}, $P_1 = 1$ s^{-2}, $P_2 = -1.2$ s^{-2}.

where the matrix D is defined as

$$\mathbf{D} = \begin{bmatrix} 0 & 0 & 1 & 0 \\ 0 & 0 & 0 & 1 \\ -K\cos(\theta_1^* - \theta_2^*) & K\cos(\theta_1^* - \theta_2^*) & -\alpha & 0 \\ K\cos(\theta_1^* - \theta_2^*) & -\gamma - K\cos(\theta_1^* - \theta_2^*) & 0 & -\alpha \end{bmatrix}. \tag{22}$$

The characteristic polynomial of matrix D is given as

$$\lambda^4 + a_1\lambda^3 + a_2\lambda^2 + a_3\lambda + a_4 = 0, \tag{23}$$

where the parameters a_1, a_2, a_3 and a_4 are given by

$$\begin{aligned} a_1 &= 2\alpha, \\ a_2 &= \alpha^2 + \gamma + 2a, \\ a_3 &= 2a\alpha + \alpha\gamma, \\ a_4 &= a\gamma, \\ a &= K\cos(\theta_1^* - \theta_2^*) = \sqrt{K^2 - P_1^2}. \end{aligned} \tag{24}$$
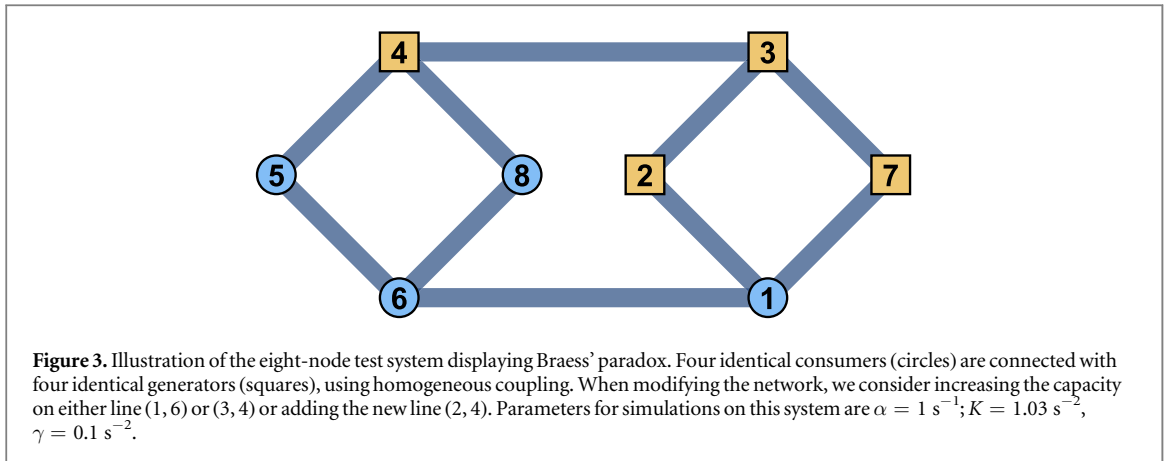
To analyze the stability of the full four-dimensional system, we need to obtain an expression for the eigenvalues. Unfortunately, a fourth or higher order polynomial does not have an easy to analyze solution so that we apply the Routh Hurwitz (RH) criterion to determine the stability [42]. The RH criterion is a method which contains the necessary and sufficient conditions for the stability of the system. Given the polynomial

$$P(\lambda) = \lambda^n + a_1\lambda^{n-1} + ... + a_{n-1}\lambda + a_n, \tag{25}$$

where the coefficients a_i are real constants, $i = 1, ..., n$, we define the n Hurwitz matrices using the coefficients a_i of the characteristic polynomial:

$$\begin{aligned} B_1 &= (a_1), \\ B_2 &= \begin{pmatrix} a_1 & 1 \\ \vdots & \\ a_3 & a_2 \end{pmatrix}..., \\ B_n &= \begin{pmatrix} a_1 & 1 & 0 & 0 & \ddots & 0 \\ a_3 & a_2 & a_1 & 1 & \ddots & 0 \\ a_5 & a_4 & a_3 & a_2 & \ddots & 0 \\ \vdots & \vdots & \vdots & \vdots & \ddots & \vdots \\ 0 & 0 & 0 & 0 & \ddots & a_n \end{pmatrix}. \end{aligned} \tag{26}$$

According to the RH criterion, all roots of the polynomial $P(\lambda)$ have negative real part if and only if the determinants of all Hurwitz matrices are positive: $\det(B_i) > 0$, for all $i = 1, 2, ..., n$ [42]. Applying the RH criterion to the steady state of our two-node system, we find that the steady state is stable if and only if the following conditions are fulfilled:

Figure 3. Illustration of the eight-node test system displaying Braess' paradox. Four identical consumers (circles) are connected with four identical generators (squares), using homogeneous coupling. When modifying the network, we consider increasing the capacity on either line $(1, 6)$ or $(3, 4)$ or adding the new line $(2, 4)$. Parameters for simulations on this system are $\alpha = 1$ s^{-1}; $K = 1.03$ s^{-2}, $\gamma = 0.1$ s^{-2}.

$$
\begin{aligned}
a_1 &> 0, \\
a_3 &> 0, \\
a_4 &> 0, \\
a_1 a_2 a_3 - a_3^2 - a_1^2 a_4 &= d > 0.
\end{aligned}
\tag{27}
$$

For the parameters used in this study, the three first conditions from (27) are always fulfilled since $\alpha, \gamma, a > 0$. Hence, the steady state is stable if and only if $d > 0$. In terms of the control parameter γ, we obtain the following inequality

$$
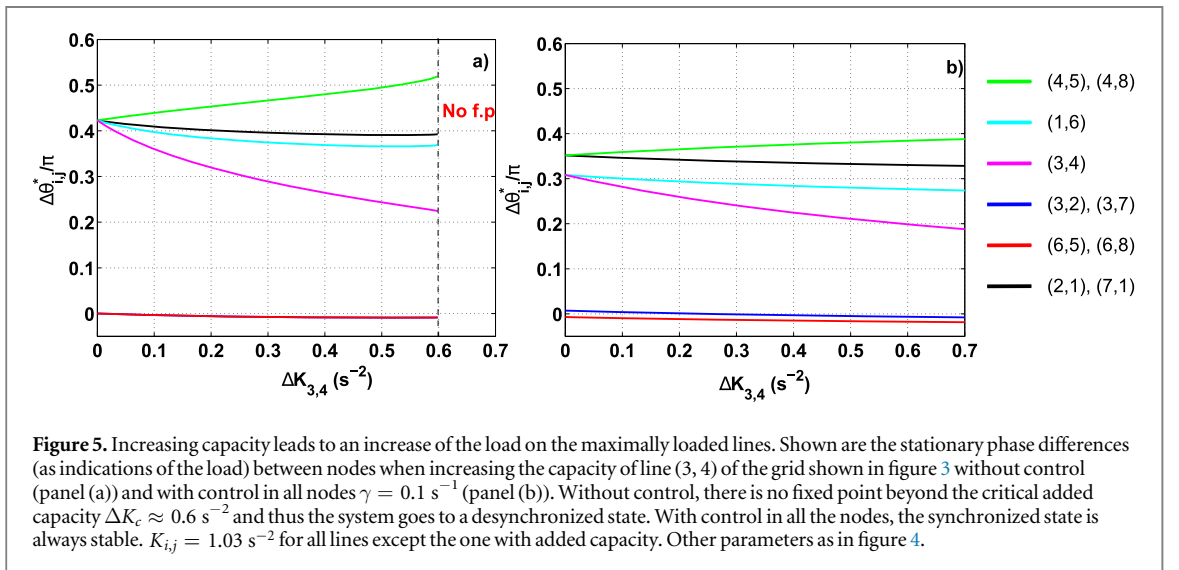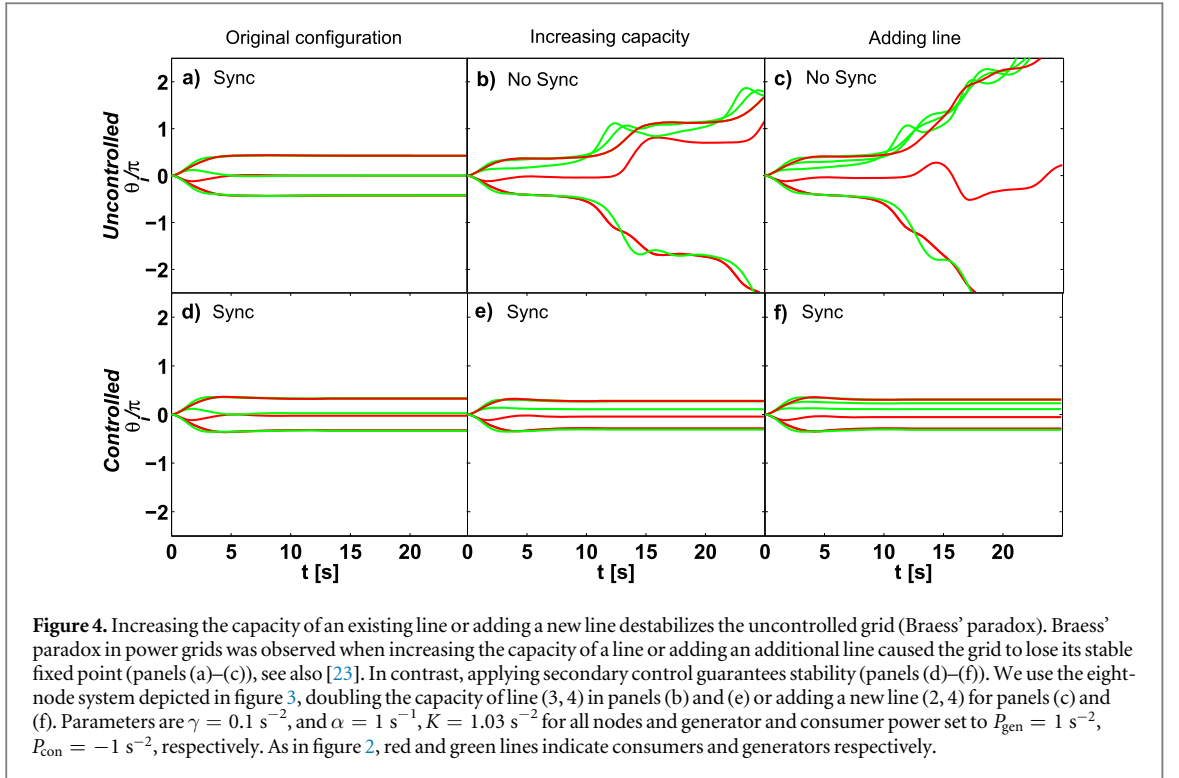\alpha^2 \gamma^2 + 2\alpha^4 \gamma + 4a\alpha^2(a + \alpha^2) > 0,
\tag{28}
$$

which again is always true; hence, as long as there is non-zero control, $\gamma > 0$, the synchronous state, whose existence is guaranteed [17], is always stable, regardless of the further specific parameters of the system, highlighting the potential of secondary control. Next, we shall investigate how secondary control interacts with changes of the network topology that lead to Braess' paradox in uncontrolled systems.

5. Braess' paradox prevented by secondary control

Adding lines to a transmission network is intuitively expected to improve its synchronization ability. However, adding certain lines instead causes the grid to lose its synchronous state. More general, the effect of adding edges to a network, thereby causing problems and decreasing performances was first predicted in 1968 for traffic networks [22] and it is since known as Braess' paradox. It was observed in traffic systems in New York, USA [43], and Stuttgart, Germany [44], when closing a street made the traffic go faster (inverse Braess' paradox).

In electric networks, Braess' paradox has been predicted in general network analysis [45], DC power flow [46] and recently in oscillator power grids [23, 24, 27]. Building additional transmission capacity under specific conditions causes Braess' paradox and thereby the grid loses its fixed point and we observe a blackout. Fortunately, not every network is susceptible to Braess' paradox. Braess' paradox can be understood in terms of the fixed point solutions as given by equation (11). Without control ($\gamma_i = 0$), the existence of fixed points is not guaranteed, as discussed in section 3, and in fact adding a line to a network can result in the equations to be overdetermined and therefore to have no solution. We interpret this in the light of the critical coupling K_c of the grid [13]: the critical coupling is defined as the minimum value of K so that for a homogeneously coupled grid, i.e. $K_{ij} = K k_{ij}$ with unweighted adjacency matrix $\mathbf{k}$, the algebraic equations (11) with $\gamma = 0$ have at least one solution. Thereby, K_c gives the minimum capacity necessary to synchronize the grid. Adding a line or increasing the capacity of an existing line effectively may increase the critical coupling K_c [23]. Increasing K_c means the fixed point can only be restored by increasing the capacity K for all lines. Besides, even if the fixed point solution exists after a modification of the network, the network eigenvalues μ_i might have changed so that the available fixed point became unstable.

To study the effect of Braess' paradox in more detail, we investigate an example network composed of eight nodes, where adding one additional transmission line or increasing the capacity of an existing line leads to a desynchronization of the network [24]. The network is shown in figure 3. The grid is such that generation and consumption are not evenly distributed, for instance, generator node 4 is connected to consumer nodes 5 and 8 while generator node 3 is not connected to any consumer. In figure 4, we plot the time evolution of the phase of each node for the original uncontrolled network, compared to the controlled network, in particular when modifying the network by increasing the capacity of an existing line or adding a new line.

Figure 4. Increasing the capacity of an existing line or adding a new line destabilizes the uncontrolled grid (Braess' paradox). Braess' paradox in power grids was observed when increasing the capacity of a line or adding an additional line caused the grid to lose its stable fixed point (panels (a)–(c)), see also [23]. In contrast, applying secondary control guarantees stability (panels (d)–(f)). We use the eight-node system depicted in figure 3, doubling the capacity of line (3, 4) in panels (b) and (e) or adding a new line (2, 4) for panels (c) and (f). Parameters are $\gamma = 0.1$ s^{-2}, and $\alpha = 1$ s^{-1}, $K = 1.03$ s^{-2} for all nodes and generator and consumer power set to $P_{\text{gen}} = 1$ s^{-2}, $P_{\text{con}} = -1$ s^{-2}, respectively. As in figure 2, red and green lines indicate consumers and generators respectively.

Figure 5. Increasing capacity leads to an increase of the load on the maximally loaded lines. Shown are the stationary phase differences (as indications of the load) between nodes when increasing the capacity of line (3, 4) of the grid shown in figure 3 without control (panel (a)) and with control in all nodes $\gamma = 0.1$ s^{-1} (panel (b)). Without control, there is no fixed point beyond the critical added capacity $\Delta K_c \approx 0.6$ s^{-2} and thus the system goes to a desynchronized state. With control in all the nodes, the synchronized state is always stable. $K_{i,j} = 1.03$ s^{-2} for all lines except the one with added capacity. Other parameters as in figure 4.

Let us review the results in detail, starting with the original network without control. As shown in panel (a), after a short transient, the original network enters a phase-locked state where all machines run stably in synchrony. The stationary power flux through line (i, j) is given by $F_{ij}^* = K_{i,j} \sin(\Delta\theta_{i,j}^*)$ where $\Delta\theta_{i,j}^* = \theta_i^* - \theta_j^*$ is the stationary phase difference. The stationary phase differences can be obtained from the fixed point given by equation (11) using Newton's method. In the following, we will mainly focus on the phase differences as indicators of how the flows are evolving and which lines have to carry additional load. As shown in figure 5 a for the steady state of the original configuration ($\Delta K_{3,4} = 0$) lines (3, 2), (3, 7), (6, 5) and (6, 8) carry no load ($\Delta\theta_{i,j}^* = F_{i,j}^* = 0$) while all other lines have identical load. Thus, the total power generated by node 3 goes to node 4 and from there it feeds the consumer nodes 5 and 8. Conversely, the power generated by nodes 2 and 7 goes to consumer 1, where half is consumed and half is fed to node 6. The steady state can be seen as composed of two subgrids, one being the mirror of the other. Let us call subgrid $\mathcal{S}_A$ the one composed by nodes 3, 4, 5 and 8 and $\mathcal{S}_B$ the one composed by other nodes.

Now, consider an increase in the capacity of line (3, 4), connecting two generator nodes, by ΔK without applying any control $\gamma = 0$. From a dynamical point of view, the capacity increase translates into a larger coupling coefficient between nodes 3 and 4. As a consequence, the phase difference between them decreases, as

Figure 6. Introducing control guarantees non-zero μ^{m} and thereby negative dynamical eigenvalues $\mathrm{Re}(\lambda^{\mathrm{m}})$. We display the largest Laplacian eigenvalues μ^{m} as a function of the added capacity of line (3, 4) in panel (a) and the largest non-zero Lyapunov exponent $\mathrm{Re}[\lambda^{\mathrm{m}}]$ in panel (b). Black lines indicate the case without control ($\gamma = 0$) and blue lines the case with control in all nodes ($\gamma = 0.1 \text{ s}^{-2}$). Parameters as in figure 5.

shown in figure 5(a) (magenta line). However, this has a side effect: phase differences $\Delta\theta_{4,5}^* = \Delta\theta_{4,8}^*$ increase (green line) as does the power flow on lines (4, 5) and (4, 8), $F_{4,5}^* = F_{4,8}^* > 1 \text{ s}^{-2}$. The power arriving from node 4 to consumers 5 and 8 is slightly larger than their consumption, thus the remaining power is fed to node 6 and the phase differences $\Delta\theta_{6,5}^* = \Delta\theta_{6,8}^*$ (red line) are no longer 0. They are slightly negative, signaling a weak flow towards consumer 6. Hence, node 6 no longer gets all the power from node 1 and $\Delta\theta_{1,6}^*$ decreases (cyan line). The flow send to consumer 1 by generators 2 and 7 is also reduced, meaning that phases $\Delta\theta_{2,1}^* = \Delta\theta_{7,1}^*$ slightly decrease (black line). Finally, since now generators 2 and 7 feed less power to node 1, the remaining power is send to node 3 and the phases $\Delta\theta_{3,2}^* = \Delta\theta_{3,7}^*$ (blue line) are no longer 0, rather slightly negative, indicating a weak flow towards node 3. Thus, the increase of capacity has induced a weak power flow between the two subgrids. Furthermore, it has broken the mirror symmetry between the subgrids. Comparing the flows with the original ones, the difference can be seen as a weak overall counter-clockwise flow. For the lines for which the original flow was in the opposite direction to this newly induced flow, the effect of the added capacity is beneficial since the flow is actually reduced. However, lines (4, 5) and (4, 8), for which the original flow has the same direction as the induced overall flow, have to carry a larger load. Eventually lines (4, 5) and (4, 8) reach the maximum power they can deliver and at $\Delta K_c \sim 0.6 \text{ s}^{-2}$ the system does no longer have a fixed point.

We may also investigate this loss of synchrony in terms of the stability analysis performed in section 3. Figure 6 shows the real part of the largest non-zero Lyapunov exponent $\mathrm{Re}[\lambda^{\mathrm{m}}]$ and the corresponding eigenvalue of the Laplacian matrix μ^{m} (black lines). For a small amount of added capacity, the overall effect is positive: μ^{m} increases, thus $\mathrm{Re}(\lambda^{\mathrm{m}})$ decreases and therefore the stability of the synchronized solution is improved, as intuitively expected. For $\Delta K_{3,4} = 0.05 \text{ s}^{-2}$, μ^{m} reaches $1/4$ so that λ^{m} becomes complex and $\mathrm{Re}(\lambda^{\mathrm{m}})$ remains clamped at $-1/2$, which is the most negative value it can take. As the capacity is further increased, μ^{m} reaches a maximum at $\Delta K = 0.16 \text{ s}^{-2}$ and then decreases. For $\Delta K_{3,4} = 0.32 \text{ s}^{-2}$, $\mu^{\mathrm{m}} < 1/4$ and $\mathrm{Re}(\lambda^{\mathrm{m}})$ starts to increase. Finally at $\Delta K_{3,4} = \Delta K_c$, $\mu^{\mathrm{m}} = 0$ and $\mathrm{Re}(\lambda^{\mathrm{m}}) = 0$. Thus, the fixed point is stable while it exists and at ΔK_c the system undergoes a saddle node bifurcation, losing the stable fixed point, which signals the Braess' paradox for this system. For $\Delta K_{3,4} > \Delta K_c$ the system enters a desynchronized regime, as shown in figure 4(b) and [23].

Similar effects can be triggered by an increase of the capacity of line (1, 6). In this case, the weak overall flow is clockwise, overloading lines (2, 1) and (7, 1) and the synchronized state disappears again at $\Delta K_c \approx 0.6 \text{ s}^{-2}$. Finally, adding a new line, e.g., (2, 4) alters the topology of the grid and without control, there is no fixed point anymore and the grid desynchronizes as shown in figure 4(c) and [23].

Is Braess' paradox still present after adding secondary control? Let us consider the same eight-node network and the same cases as before but now with control in all the nodes $\gamma_i = \gamma > 0$. As shown in figures 4(e) and (f), controlling the network guarantees a stable state even after doubling the capacity of line (3, 4) or adding a new line (2, 4), thereby preventing Braess' paradox.

As indicated in section 3, when control is included in all nodes, there is always a fixed point solution. Even if the transmission capacity K_{ij} is insufficient or would normally cause Braess' paradox, the term $-\gamma_i\theta_i^*$ in equation (11) balances both sides of the equation and guarantees a solution. In fact

$$\Delta P_i^* = -\gamma_i\theta_i^* \qquad (29)$$

is the power provided by the secondary control in the stationary regime. The effective power generated/consumed at each node in the stationary regime is given by
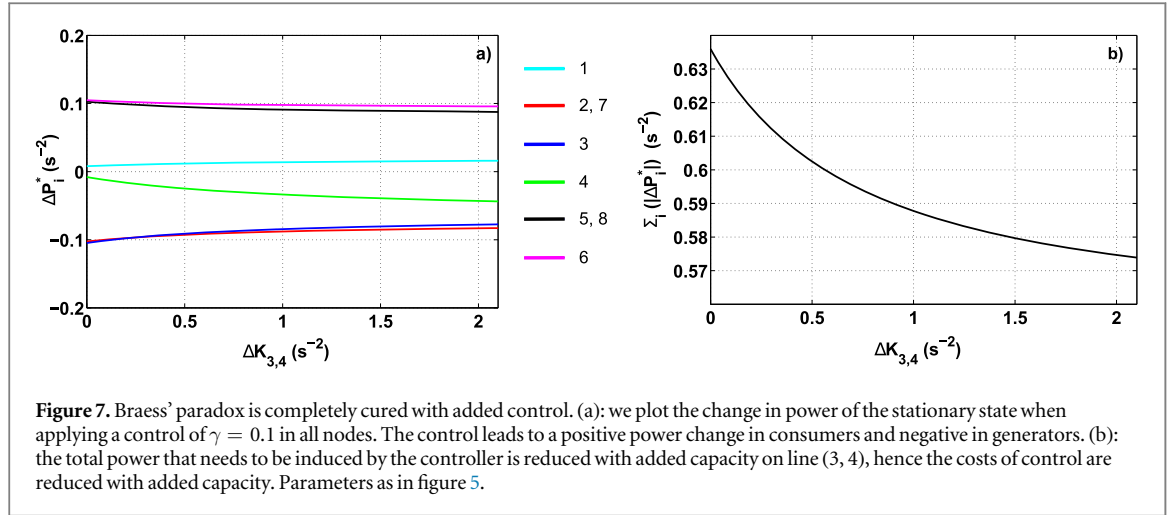
Figure 7. Braess' paradox is completely cured with added control. (a): we plot the change in power of the stationary state when applying a control of $\gamma = 0.1$ in all nodes. The control leads to a positive power change in consumers and negative in generators. (b): the total power that needs to be induced by the controller is reduced with added capacity on line (3, 4), hence the costs of control are reduced with added capacity. Parameters as in figure 5.

$$P_i^{\text{eff}} = P_i + \Delta P_i^*. \tag{30}$$

Thereby, we do not need to increase the capacity of all lines because the control reduces the total power flow in the system.

We illustrate this for a two-node system with $\gamma_1 = \gamma_2 = \gamma$. The critical coupling is then given as

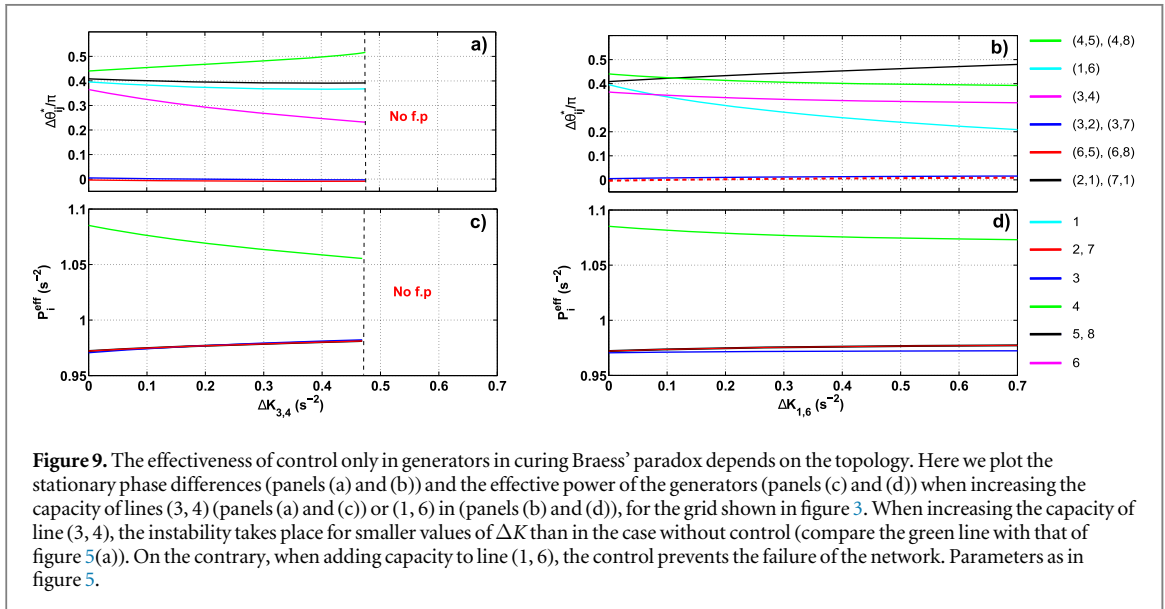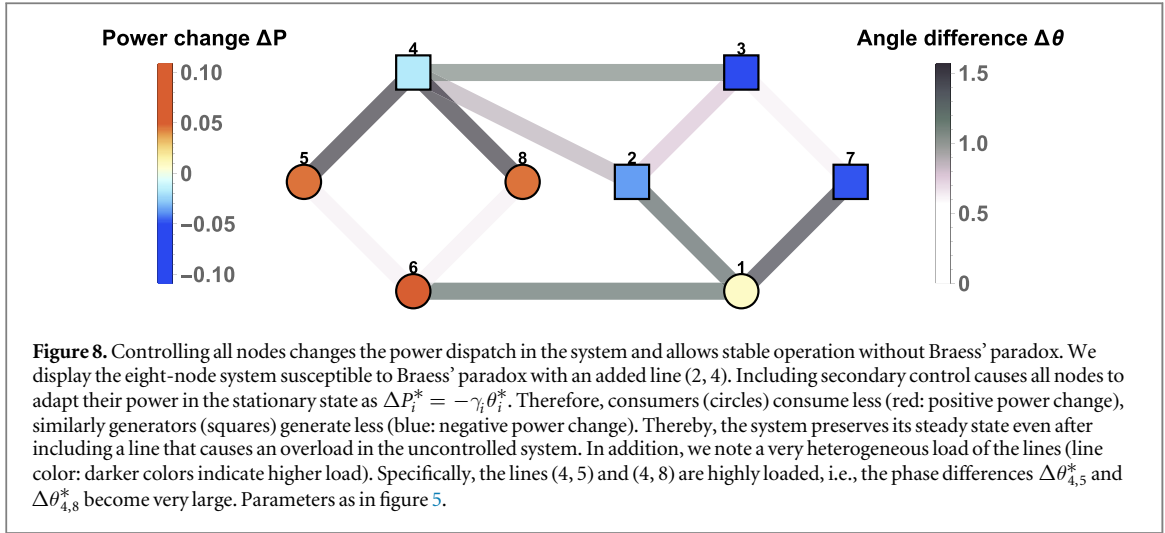$$K_c^{\text{New}} = K_c - \gamma \Delta\theta/2, \tag{31}$$

i.e. the controller reduces the load on the lines, enabling a fixed point with lower capacity. Following the same argumentation, secondary control also cures Braess' paradox which would otherwise require an increase of the transmission capacity.

To better understand how the controller stabilizes the network, we plot the stationary change of power with respect to the nominal values ΔP_i^* as the capacity of line (3, 4) increases in figure 7(a). Consider first the original network, $\Delta K_{3,4} = 0$. The added control changes the effective power of each node. With control, generators have negative and consumers positive power change, i.e., consumption is reduced as well as generation. As a consequence, the power flow through the loaded lines is reduced and the phase differences are smaller than in the uncontrolled case. Furthermore, the control induces a (small) flow between the two subgrids. This steady state is more robust with respect to perturbations than the uncontrolled case for two reasons: first, the range for which $\text{Re}(\lambda^m)$ is negative now extends to negative values of μ^m as shown in figure 1(b). Second, as shown in figure 6, for this steady state $\mu^m = 0.447$, which is in fact larger than that of the steady state without control. As a consequence $\text{Re}[\lambda^m] = -1/2$ which is way below the value for the uncontrolled case and is the most negative value it can take.

As capacity is added to line (3, 4), $\Delta\theta_{3,4}^*$ decreases as expected, see the magenta line in figure 5(b), thus control gradually decreases the effective power of node 4, while increasing that of the other generators so that effective power in the different generator nodes becomes more similar as shown in figure 7. In the same way, control gradually decreases the consumption of node 1, while increasing the consumption of the other nodes. Although the phase differences $\Delta\theta_{4,5}^* = \Delta\theta_{4,8}^*$ increase, lines (4, 5) and (4, 8) never get overloaded. As shown in figure 6, blue lines, as additional capacity is added, the eigenvalue μ^m keeps increasing and the largest dynamical eigenvalue $\text{Re}[\lambda^m]$ remains clamped at $-1/2$, signaling maximum stability. Therefore, the synchronized steady state is always stable, curing Braess' paradox.

What is the cost of this cure? By introducing the secondary control, all controlled nodes have to provide control power in form of ΔP_i^*. The more power that has to be provided, the more costly the secondary controller becomes. When curing Braess' paradox, we might have just shifted the paradox from the power flow to the control costs. To analyze this, we consider the sum of the absolute values of the stationary power provided by the controlled system, $\sum_i |\Delta P_i^*|$, which can be seen as an indicator of the overall costs of control. As shown in figure 7(b), as $\Delta K_{3,4}$ increases, the overall costs, $\sum_i |\Delta P_i^*|$, do not increase, on the contrary, they decrease. Therefore, if all nodes are controlled, an increase in line capacity is beneficial, not only for the stability but also in decreasing the overall costs of control, and thus Braess' paradox is completely avoided.

Similarly, adding the new line (2, 4) with control applied to all nodes, reduces total control costs. The changes of power ΔP_i^* and the total load on the lines are visualized in figure 8. As before, generators have negative and consumers positive power change i.e., the total consumption and the total generation are decreased with respect to the uncontrolled case.

Figure 8. Controlling all nodes changes the power dispatch in the system and allows stable operation without Braess' paradox. We display the eight-node system susceptible to Braess' paradox with an added line (2, 4). Including secondary control causes all nodes to adapt their power in the stationary state as $\Delta P_i^* = -\gamma_i \theta_i^*$. Therefore, consumers (circles) consume less (red: positive power change), similarly generators (squares) generate less (blue: negative power change). Thereby, the system preserves its steady state even after including a line that causes an overload in the uncontrolled system. In addition, we note a very heterogeneous load of the lines (line color: darker colors indicate higher load). Specifically, the lines (4, 5) and (4, 8) are highly loaded, i.e., the phase differences $\Delta\theta_{4,5}^*$ and $\Delta\theta_{4,8}^*$ become very large. Parameters as in figure 5.

Figure 9. The effectiveness of control only in generators in curing Braess' paradox depends on the topology. Here we plot the stationary phase differences (panels (a) and (b)) and the effective power of the generators (panels (c) and (d)) when increasing the capacity of lines (3, 4) (panels (a) and (c)) or (1, 6) in (panels (b) and (d)), for the grid shown in figure 3. When increasing the capacity of line (3, 4), the instability takes place for smaller values of ΔK than in the case without control (compare the green line with that of figure 5(a)). On the contrary, when adding capacity to line (1, 6), the control prevents the failure of the network. Parameters as in figure 5.

6. Controlling only the generators

So far, we have assumed that all nodes in the network can be controlled. Effective consumer nodes, however, may have limited generation capacity and therefore limited control capability. Therefore, let us now assume that secondary control is only available at the nodes with positive power generation (generators), as usual in today's power grids [5]. Since the total consumption is fixed, the total generation also has to stay constant, thus the control can only redistribute the effective power delivered by the generators among them. In this case, the effectiveness of the control depends strongly on the topology, e.g. which line is getting upgraded. We consider two cases.

First, we consider an increase of the capacity of line (3, 4) by $\Delta K_{3,4}$, which without control eventually leads to Braess' paradox (figure 4(b)). Adding control in generators only does not help to improve the situation. In fact, as shown in figure 9(a) the phase differences $\Delta\theta_{4,5}^* = \Delta\theta_{4,8}^*$ increase faster with $\Delta K_{3,4}$ and the fixed point disappears at $\Delta K_c \sim 0.49$ s^{-2}, i.e. for a lower value than without control. So, controlling only the generators does not prevent Braess' paradox reliably. To understand this phenomenon, consider the original grid. Since node 4 has to feed two consumer nodes, control increases the effective power of 4, while it decreases that of the other generators, as shown in figure 9(c) at $\Delta K_{3,4} = 0$. The total power generation in subgrid $\mathcal{S}_A$ becomes smaller than in subgrid $\mathcal{S}_B$. Since consumers have a fixed power, a small net flux has to go from subgrid $\mathcal{S}_A$ to $\mathcal{S}_B$. The additional flow is transmitted through lines (6, 5) and (6, 8), which now carry a small flux towards 6 and through lines (3, 2), (3, 7) which carry flux towards 2 and 7. As a consequence, the fluxes $F_{4,5}^* = F_{4,8}^*$ become larger than in the uncontrolled case. Adding additional capacity at line (3, 4) leads to a reduction of the effective power in generator 4 and an increase of power for the other generators so that the overall net flow from subgrid
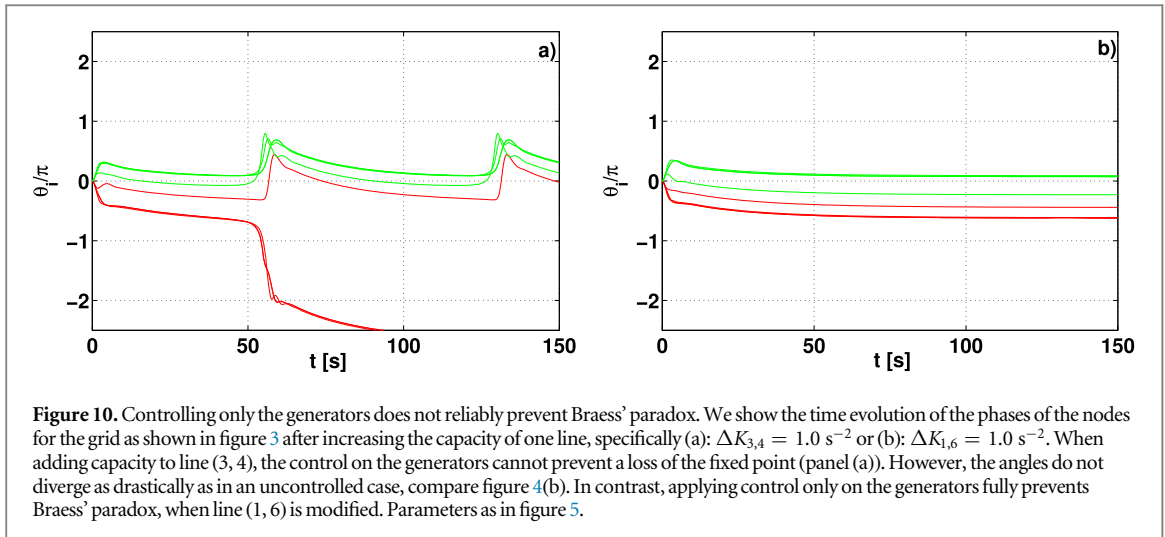
Figure 10. Controlling only the generators does not reliably prevent Braess' paradox. We show the time evolution of the phases of the nodes for the grid as shown in figure 3 after increasing the capacity of one line, specifically (a): $\Delta K_{3,4} = 1.0\ \text{s}^{-2}$ or (b): $\Delta K_{1,6} = 1.0\ \text{s}^{-2}$. When adding capacity to line (3, 4), the control on the generators cannot prevent a loss of the fixed point (panel (a)). However, the angles do not diverge as drastically as in an uncontrolled case, compare figure 4(b). In contrast, applying control only on the generators fully prevents Braess' paradox, when line (1, 6) is modified. Parameters as in figure 5.

$\mathcal{S}_A$ to $\mathcal{S}_B$ decreases. However, the added capacity, as discussed in the context of figure 5, breaks the symmetry and in fact the flow through (6, 5) and (6, 8) actually increases, while that through (3, 2), (3, 7) decreases (which can even reverse). The increasing flow arises as a combination of a flow between the subgrids for the original network and a weak counter-clockwise flow induced by the added capacity. To account for the increasing flux going through (6, 5) and (6, 8), the flux through lines (4, 5) and (4, 8), which were already quite loaded, also has to increase. Thus, with control only in generators, the angles $\Delta\theta_{4,5}^*$ and $\Delta\theta_{4,8}^*$ are larger than without control and thus instability takes place at a smaller value of ΔK_c.

Nevertheless, the oscillatory regime reached after the instability is somehow different in the cases with and without control, as shown in figure 10(a). With control, most of the nodes remain synchronized at the reference frequency and only two nodes show phase slips at a slow time scale. On the contrary, without control all nodes rotate showing phase slips at a much faster rate (compare with figure 4(b)) for the same $\Delta K_{3,4}$ noting the different time scale of both figures.

Next, we consider an increase of the capacity of line (1, 6), connecting two consumer nodes, by $\Delta K_{1,6}$. As discussed in section 5 without control, increasing $\Delta K_{1,6}$ increases the load on lines (2, 1) and (7, 1) until the system becomes unstable at $\Delta K_c \sim 0.6\ \text{s}^{-2}$, leading to Braess' paradox. Applying control exclusively to generator nodes does indeed help in this case. The range of existence of the fixed point is extended to any value of $\Delta K_{1,6}$ preventing the paradox completely, see figure 10(b). Let us analyze why here the synchronous state is stabilized while this was not the case when increasing the capacity of line (3, 4). Consider the case of no added capacity: the phase differences and the effective power delivered by each generator are the same in both cases as shown in figure 9. The phase difference for lines (2, 1) and (7, 1) (black) is smaller than that of lines (4, 5) and (4, 8) (green). This is because the control in generators increases the angles $\Delta\theta_{4,5}^*$ and $\Delta\theta_{4,8}^*$ while it decreases $\Delta\theta_{2,1}^* = \Delta\theta_{7,1}^*$, compared to the system without control. In this situation, adding extra capacity in line (1, 6) will increase the difference $\Delta\theta_{2,1}^* = \Delta\theta_{7,1}^*$ and thus the flux carried on lines (2, 1) and (7, 1). However, the added capacity will, as before, reduce the overall net flow from subgrid $\mathcal{S}_A$ to $\mathcal{S}_B$, slowing down the growth of the phase differences $\Delta\theta_{2,1}^* = \Delta\theta_{7,1}^*$. The aftermath is that lines (2, 1) and (7, 1) do not get saturated in this case and Braess paradox is avoided.

7. Discussion

The above results indicate that simple secondary control may successfully restore the grid frequency of an unbalanced power grid and is also capable of preventing Braess' paradox.

Secondary control, when applied to all nodes, improves the stability of the grid, regardless of topology, and even allows stable operation for mismatched power [1, 5, 47]. While primary control stabilizes the frequency, secondary control restores the frequency to the reference value and guarantees the existence of a stable fixed point. We have systematically computed the fixed point stability of the power grid with secondary control as a function of both the network topology and the control action. Control improves stability, increasing the range of network topologies for which the synchronized steady state is stable. Thereby, we have extended previous stability analysis of uncontrolled systems [11] or systems including secondary control restricted to balanced power [38].

Secondary control in all nodes also prevents the loss of the operational state via Braess' paradox. As shown by Witthaut and Timme [23, 24], the addition of certain transmission lines may lead to a loss of the operational state

of a power grid. Using primary control only [13] does not suffice to prevent Braess' paradox. We have now demonstrated that secondary control prevents the desynchronization in networks prone to Braess' paradox if all nodes, i.e., effective consumers and generators alike, are controlled (figures 4 and 8). The control reduces the total amount of net power generated and consumed at each node of the grid, guaranteeing that the transmitted power does not exceed the transmission capacity. Thereby, it offers a trade-off between grid extension and investments in control, assuming some amount of local generation is possible. Once secondary control is implemented in all nodes, subsequent line capacity increases are beneficial, both for stability and also in decreasing the overall power delivered by the control and thus its cost, fully avoiding Braess' paradox.

In today's grid, secondary control is implemented only in power plants. Thus, nodes with generation much larger than consumption, i.e., generator nodes, have a large control capability while nodes in which consumption is larger than generation (effective consumer nodes) have very little, if any, control capability. If only generator nodes are controlled, then the control will only redistribute the effective power delivered by the generators among them and as a consequence the grid topology determines the benefits of the controller. We have observed that if the capacity of a line connecting two generator nodes is increased, the control does not prevent Braess' paradox. On the contrary, in the case of increasing the capacity of a line connecting two consumer nodes, secondary control is capable of redistributing the power flow so that no lines are overloaded and the paradox is avoided.

Concluding, using secondary control on all nodes in a network improves its stability and robustness with respect to dynamical and topological perturbations. If control is mainly available in generator nodes, the effectiveness of the control depends strongly on the topology of the network. This stresses the importance of involving consumers, e.g. via demand control schemes or local generation (prosumers) in future grids [15, 16, 28, 48]. Alternatively, other options to provide secondary control at the consumer side, e.g. by using distributed storage or back-up generation, have to be considered. Finally, further research is necessary to extend our results, e.g., to alternative control mechanisms. One example is to allow $\tau > 0$ in equation (9), i.e., making the power provided by each node explicitly time-dependent.

Acknowledgments

ORCID iDs

Eder Batista Tchawou Tchuisseu ⓘ https://orcid.org/0000-0003-3160-4635
Damià Gomila ⓘ https://orcid.org/0000-0002-3500-3434
Pere Colet ⓘ https://orcid.org/0000-0002-5992-6292
Dirk Witthaut ⓘ https://orcid.org/0000-0002-3623-5341
Marc Timme ⓘ https://orcid.org/0000-0002-5956-3137
Benjamin Schäfer ⓘ https://orcid.org/0000-0003-1607-9748

References

[1] Kundur P, Balu N J and Lauby M G 1994 *Power System Stability and Control* vol 7 (New York: McGraw-Hill)
[2] Brummitt C D, Hines P D H, Dobson I, Moore C and D'Souza R M 2013 *Proc. Natl Acad. Sci.* **110** 12159
[3] Kovacevic R M, Pflug G C and Vespucci M T 2013 *Handbook of Risk Management in Energy Production and Trading* (Berlin: Springer)
[4] Schäfer B, Beck C, Aihara K, Witthaut D and Timme M 2018 *Nat. Energy* **3** 119
[5] Machowski J, Bialek J and Bumby J 2011 *Power System Dynamics: Stability and Control* (New York: Wiley)
[6] Boyle G 2004 *Renewable Energy* (Oxford: Oxford University Press)
[7] Sims R *et al* 2011 *IPCC Special Report on Renewable Energy Sources and Climate Change Mitigation* ed O Edenhofer *et al* (Cambridge: Cambridge University Press)
[8] Ueckerdt F, Brecha R and Luderer G 2015 *Renew. Energy* **81** 1
[9] Filatrella G, Nielsen A H and Pedersen N F 2008 *Eur. Phys. J.* B **61** 485
[10] Rohden M, Sorge A, Timme M and Witthaut D 2012 *Phys. Rev. Lett.* **109** 064101

[11] Motter A E, Myers S A, Anghel M and Nishikawa T 2013 *Nat. Phys.* **9** 191

[12] Dörfler F and Bullo F 2014 *Automatica* **50** 1539

[13] Manik D, Witthaut D, Schäfer B, Matthiae M, Sorge A, Rohden M, Katifori E and Timme M 2014 *Eur. Phys. J. Spec. Top.* **223** 2527

[14] Rohden M, Sorge A, Witthaut D and Timme M 2014 *Chaos* **24** 013123

[15] Schäfer B, Matthiae M, Timme M and Witthaut D 2015 *New J. Phys.* **17** 015002

[16] Schäfer B, Grabow C, Auer S, Kurths J, Witthaut D and Timme M 2016 *Eur. Phys. J. Spec. Top.* **225** 569

[17] Weitenberg E, Jiang Y, Zhao C, Mallada E, De Persis C and Dörfler F 2018 *IEEE Transactions on Automatic Control*

[18] Ipakchi A and Albuyeh F 2009 *IEEE Power Energy Mag.* **7** 52

[19] 2012 50 Hertz Transmission GmbH and Amprion and TenneT TSO and TransnetBW, Netzentwicklungplan Strom http://netzentwicklungsplan.de

[20] Fürsch M, Hagspiel S, Jägemann C, Nagl S, Lindenberger D and Tröster E 2013 *Appl. Energy* **104** 642

[21] Schäfer B, Witthaut D, Timme M and Latora V 2018 *Nat. Commun.* **9** 1975

[22] Braess D 1968 *Math. Methods Oper. Res.* **12** 258

[23] Witthaut D and Timme M 2012 *New J. Phys.* **14** 083036

[24] Witthaut D and Timme M 2013 *Eur. Phys. J.* B **86** 377

[25] Nagurney L S and Nagurney A 2016 *Europhys. Lett.* **115** 28004

[26] Coletta T and Jacquod P 2016 *Phys. Rev.* E **93** 032222

[27] Fazlyaba M, Dörfler F and Preciadoa V M 2017 *Automatica* **84** 181

[28] Tchawou Tchuisseu E B, Gomila D, Brunner D and Colet P 2017 *Phys. Rev.* E **96** 022302

[29] Heide D, Bremen L V, Greiner M, Hoffmann C, Speckmann M and Bofinger S 2010 *Renew. Energy* **35** 2483

[30] Milan P, Wächter M and Peinke J 2013 *Phys. Rev. Lett.* **110** 138701

[31] Saadat H 2002 *Power Systems Analysis* (New York: McGraw-Hill)

[32] Anderson P M and Fouad A A 2008 *Power System Control and Stability* (New York: Wiley)

[33] Grzybowski J, Macau E and Yoneyama T 2016 *Chaos* **26** 113113

[34] Wang C, Grebogi C and Baptista M S 2016 *Chaos* **26** 093119

[35] Simpson-Porco J W, Dörfler F and Bullo F 2012 *IFAC Proc. Vol.* **45** 264

[36] Hammid A T, Hojabri M, Sulaiman M H, Abdalla A N and Kadhim A A 2016 *J. Telecommun., Electron. Comput. Eng.* **8** 47

[37] Dongmo E D, Colet P and Woafo P 2017 *Eur. Phys. J.* B **90** 6

[38] Martyr R, Schaefer B, Beck C and Latora V 2018 arXiv:1802.06647

[39] Dörfler F, Chertkov M and Bullo F 2013 *Proc. Natl Acad. Sci.* **110** 2005

[40] Pecora L M and Carroll T L 1998 *Phys. Rev. Lett.* **80** 2109

[41] Wang B, Suzuki H and Aihara K 2016 *Sci. Rep.* **6** 26596

[42] Xie L 2011 *Int. J. Mod. Educ. Comput. Sci.* **3** 38

[43] Kolata G 1990 What if they closed 42d street and nobody noticed? *The New York Times* **1990** 1001038

[44] Knödel W 2013 *Graphentheoretische Methoden und ihre Anwendungen* vol 13 (Berlin: Springer)

[45] Motter A E 2004 *Phys. Rev. Lett.* **93** 098701

[46] Labavić D, Suciu R, Meyer-Ortmanns H and Kettemann S 2014 *Eur. Phys. J. Spec. Top.* **223** 2517

[47] Wood A J, Wollenberg B F and Sheblé G B 2013 *Power Generation, Operation and Control* (New York: Wiley)

[48] Fang X, Misra S, Xue G and Yang D 2012 *IEEE Commun. Surv. Tutorials* **14** 944